






Journal of Experimental Biology and Agricultural Sciences

<http://www.jebas.org>

ISSN No. 2320 – 8694

Molecular Interactions of Mycobacterial Transporter for Novel Antimicrobial Strategies

Arathi Radhakrishnan¹ , Manisha Gurnani² , Priyanka Gopi⁴ , Abhishek Chauhan³ ,
Prateek Pandya⁴ , Raj Kishor Kapardar⁵ , Rajpal Srivastav^{1*} 

¹Amity Institute of Biotechnology, Amity University Uttar Pradesh, Noida, India.

²Amity Institute of Environmental Science, Amity University Uttar Pradesh, Noida, India.

³Amity Institute of Environmental Toxicology and Safety Management, Amity University Uttar Pradesh, Noida, India

⁴Amity Institute of Forensic Sciences, Amity University Uttar Pradesh, Noida, India

⁵Microbial Division, The Energy and Resources Institute, New Delhi, India

Received – October 16, 2024; Revision – January 30, 2025; Accepted – February 09, 2025

Available Online – March 05, 2025

DOI: [http://dx.doi.org/10.18006/2025.13\(1\).59.71](http://dx.doi.org/10.18006/2025.13(1).59.71)

KEYWORDS

Mycobacterium tuberculosis

Efflux Transporter

Protein-Ligand Interactions

MATE Transporter

Drug repurposing

ABSTRACT

Efflux mechanisms for extruding antimicrobials, mediated by multidrug transporters, are key contributors to multidrug resistance in mycobacteria. The current study focused on molecular interaction analysis of *Mycobacterium tuberculosis* multidrug transporter implicated in multidrug and antimicrobial resistance. We screened a library of efflux transporter inhibitors against the protein structure to identify a lead compound that can potentially inhibit the transporter significantly. The efflux transporter sequence was modeled based on crystallized templates using protein structure prediction and molecular docking. The analysis deduced molecular interactions and critical binding residues that can be targeted as novel biotherapeutics strategies against multidrug transporters of mycobacteria. This study paves the way for targeting multidrug and antimicrobial resistance in the mycobacteria, offering hope for developing effective treatments.

* Corresponding author

E-mail: rsrivastav2@amity.edu (Rajpal Srivastav)

Peer review under responsibility of Journal of Experimental Biology and Agricultural Sciences.

Production and Hosting by Horizon Publisher India [HPI]
(<http://www.horizonpublisherindia.in/>).
All rights reserved.

All the articles published by [Journal of Experimental Biology and Agricultural Sciences](#) are licensed under a [Creative Commons Attribution-NonCommercial 4.0 International License](#) Based on a work at www.jebas.org.



1 Introduction

In 2023, the World Health Organization (WHO) reported approximately 1.25 million deaths from tuberculosis (TB), making it the leading infectious disease killer, surpassing COVID-19 (Goletti et al. 2025; WHO 2024). The increase in TB cases, along with the emergence of multidrug-resistant TB (MDR-TB) and extensively drug-resistant TB (XDR-TB), highlights the urgent need for innovative therapeutic strategies, especially in high-burden countries such as India, China, Indonesia, Philippines, and Pakistan (Monedero-Recuero et al. 2021; Wilczek et al. 2023).

Mycobacterium tuberculosis (Mtb) employs various mechanisms to evade and tolerate antimicrobial agents (Andre et al. 2017; Srivastav et al. 2014). Its waxy, impermeable cell wall limits drug penetration (Yang et al. 2023), and the upregulation of efflux transporters actively expels drugs from the cell (Campollatano et al. 2023). Genetic mutations, such as those in the *rpoB* gene, confer resistance to rifampicin (Traoré et al. 2023; Andre et al. 2017), while dormancy decreases antibiotic susceptibility (Shan Chang and Guan 2021; Day et al. 2024). Within the host, Mtb evades immune defenses by inhibiting the fusion of phagosomes and lysosomes (Maphasa et al. 2021) and impairing cytokine signaling and granuloma formation (Peddireddy et al. 2017). Efflux transporters significantly contribute to multidrug tolerance by reducing effective intracellular drug concentrations (Tyagi et al. 2022; Ghajavand et al. 2019). MDR strains resist first-line drugs like isoniazid and rifampicin, while XDR strains also resist second-line agents such as fluoroquinolones and aminoglycosides (“WHO Results Report 2020-2021,” n.d.; Seung et al. 2015). Additionally, various uncharacterized efflux transporters in Mtb may be

associated with antimicrobial resistance (Huang et al. 2022; Zgurskaya 2021). Therefore, targeting these transporters presents a promising therapeutic strategy against mycobacterial infections (Klukovits and Krajcsi 2015; Rodrigues et al. 2020).

Efflux transporters are classified into major protein families based on their distinct structural and functional characteristics, as illustrated in Figure 1. The Mtb genome encodes at least 65 putative drug efflux pumps from various families, significantly contributing to antimicrobial resistance (Mishra and Daniels 2013; Black et al. 2014). Among these, four families, i.e., ABC, MFS, SMR, and MATE, have demonstrated efflux activities in Mtb, actively removing first- and second-line TB drugs, thereby diminishing their effectiveness (Long et al. 2024). Mycobacterial efflux transporters abundance and broad substrate specificity contribute to high intrinsic drug tolerance (Poulton and Rock 2022; Sharma et al. 2023).

MATE transporters are known for their poly specificity, which allows them to extrude various drugs and contributes to the antimicrobial resistance observed in mycobacterial species, including *M. tuberculosis* (Mishra and Daniels 2013). MATE is classified as a multidrug transporter. The Rv2836c protein, identified as a potential member of the MATE family of efflux transporters, may play a role in mycobacterial drug resistance. Although its structure has not been determined experimentally, it is predicted to have MATE transporters typical 12-transmembrane domain characteristic (Roberts 2022). Stress factors, including exposure to antimicrobials, may induce the expression of this multidrug transporter. However, the regulatory mechanisms governing this expression are not yet fully understood. Targeting

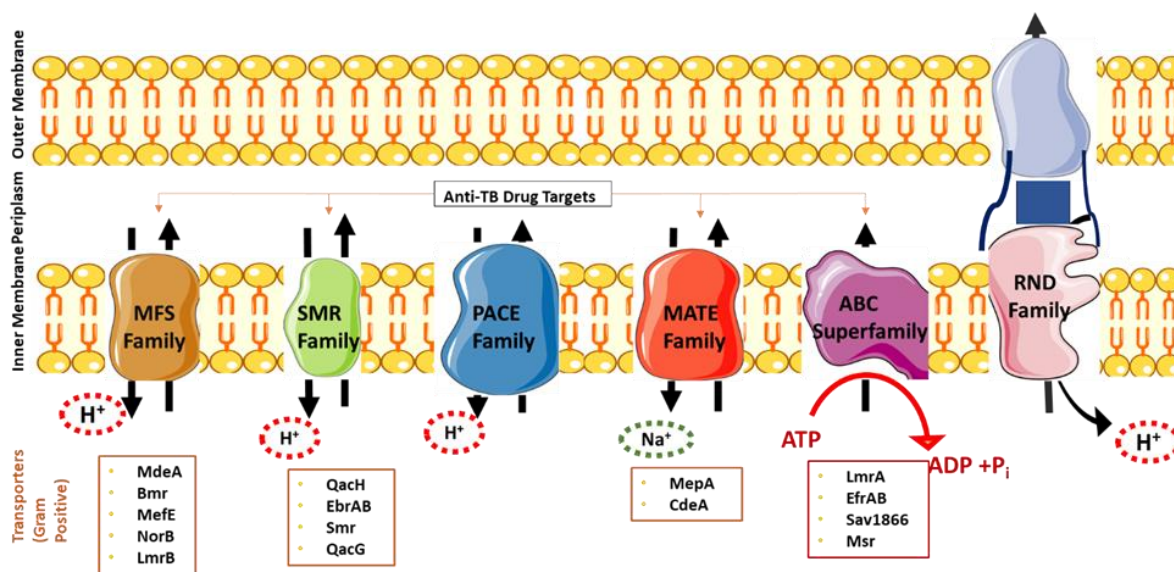


Figure 1 Illustration showing the different classes of efflux transporters: proteins that expel harmful substances and antibiotics from bacterial cells. This image highlights major efflux systems identified in Gram-positive organisms, which are significant in antimicrobial resistance (As per Athar et al. 2023; Henderson et al. 2021; Hassan et al. 2018)).

Rv2836c could potentially enhance the efficacy of antimicrobials by modifying intracellular drug concentrations. Therefore, the current study aims to investigate the molecular interactions between potential drug candidates and the Mtb MATE transporter using an *in-silico* approach.

2 Materials & Methods

2.1 Homology Modeling and Validation of Protein

After completing the literature review, it was found that the tuberculosis Multidrug and Toxic Compound Extruder (MATE) crystal structure is not available in the PDB database. Consequently, homology modeling was performed using Modeller and the MODBASE tool (<https://modbase.compbio.ucsf.edu/modweb/>) based on the existing structure of the MATE family multidrug resistance transporter Aq_128 (PDB ID: 6FV6). The modeled structure was then minimized using the SPDBV software tool version 4.1.0. Next, structure alignment was conducted in Biovia Discovery Studio Visualiser client version 2021 to ensure no significant deviations from the reference structure. The modeled Protein was validated using the SAVES server (<https://saves.mbi.ucla.edu/>) and the Ramachandran plot. Finally, the binding cavity of the modeled Protein was analyzed using a depth server (<https://cospi.iiserpune.ac.in/depth>).

2.2 Ligand Data Set Preparation

A selection of compounds was developed to target proton channels and multidrug transporters, emphasizing inhibiting efflux pumps. However, only a limited number of existing efflux pump inhibitors were identified, and none have been tested against the MATE transporter in *M. tuberculosis* (Mtb). Consequently, computational screening was conducted to evaluate the efficacy of these inhibitors on the catalytic site of the MATE protein. The SDF files for these compounds were retrieved from PubChem (<https://pubchem.ncbi.nlm.nih.gov/>). Legend files were generated using the Open Babel software (O'Boyle et al. 2011) and a Raccoon Python script (Forli et al. 2016).

2.3 Molecular Docking and Screening

The receptor protein was processed using AutoDock tools for grid generation. The residues from the DEPTH server were a guiding reference for this grid generation. An exhaustiveness setting of 9 was applied. The binding pose exhibiting the most favorable negative binding energy (BE) value identified the most promising results. A Python script was utilized to calculate the optimal docking score of the MATE transporter protein with the transporter inhibitor to screen potential drug molecules. This analysis and screening aimed to establish a dataset of potential drug candidates.

2.4 Drug-Likeness and ADMET Prediction

Web tools with effective internal methods, such as pkCSM (<https://biosig.lab.uq.edu.au/pkcs/>) and BOILED-Egg from SWISS ADME (<http://www.swissadme.ch/>), have been utilized to create robust predictive models for the physicochemical properties, pharmacokinetics, and drug-like characteristics of top-screened compounds. The SMILES representation of the lead molecule was obtained from the PubChem database, while these servers provided the values for Absorption, Distribution, Metabolism, and Excretion.

2.5 Molecular Dynamics

Molecular dynamics simulations were performed on the Google Colab server using NAMD GPU 2.0 (Phillips et al. 2020; Gopi et al. 2023). The docked pose with the highest affinity, indicated by the lowest docking score, was selected for simulation. Topology and parameter files for the Protein and ligand were generated using CHARMM GUI and VMD 1.9.3 (Lee et al. 2016). The complexes were solvated with the TIP3P water model and neutralized with sodium and chloride ions. The protein-drug complex was minimized for 10000 steps, followed by NVT equilibration and NPT equilibration for 1 ns each while maintaining a pressure of 1.02 atm and a temperature of 310 K. A final production run of 100 ns was conducted for both systems using the CHARMM36 force fields, and VMD 1.9.3 was used to analyze the trajectories (Humphrey et al. 1996).

2.6 MM/PBSA

The Poisson-Boltzmann Surface Area (PBSA) algorithm was employed to analyze the protein-drug complex's binding free energy (ΔG_{bind}). We utilized 1,500 snapshots from the trajectories over a 100 ns simulation, conducting the calculations with the CaFE plugin in VMD 1.9.3 (Humphrey et al. 1996). The internal dielectric constant for MM/PB was set to 1.0, while the external dielectric constant was set to 80.0. Poisson-Boltzmann calculations used the Adaptive Poisson-Boltzmann Solver (APBS) to define the boundary conditions and charges. The solvent-accessible surface area was computed with a surface tension of 0.00542 and a surface offset of 0.92 (Table 2).

3 Results and Discussion

3.1 Homology Modeling of MATE transporter protein and ligand preparation

After analyzing various transporters, we found that the MATE protein is conserved across different mycobacterial species. We conducted modeling of the MATE transporter protein based on the existing structure of the MATE family transporter Aq_128 (PDB ID: 6FV6) (Zhao et al. 2021). We performed a sequence alignment

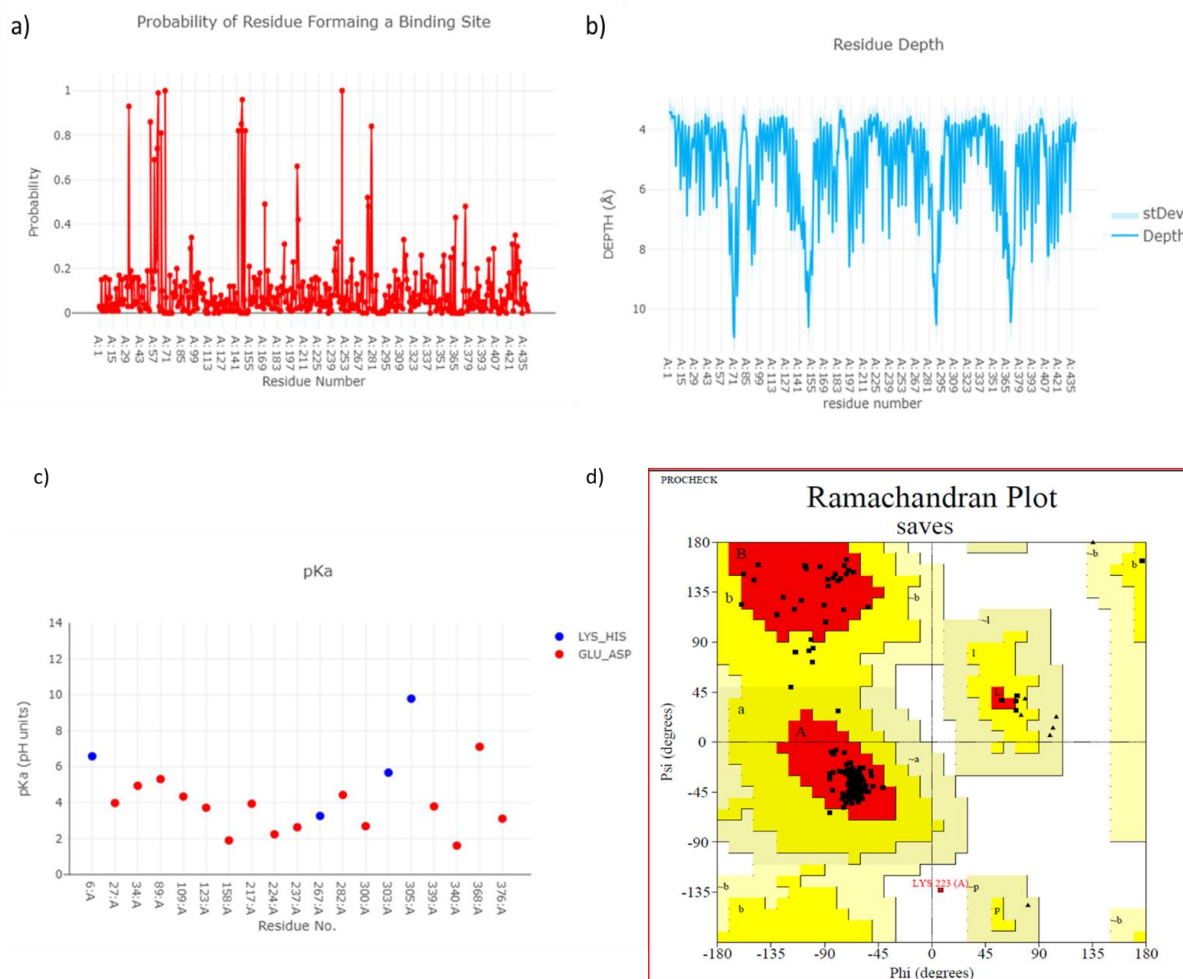
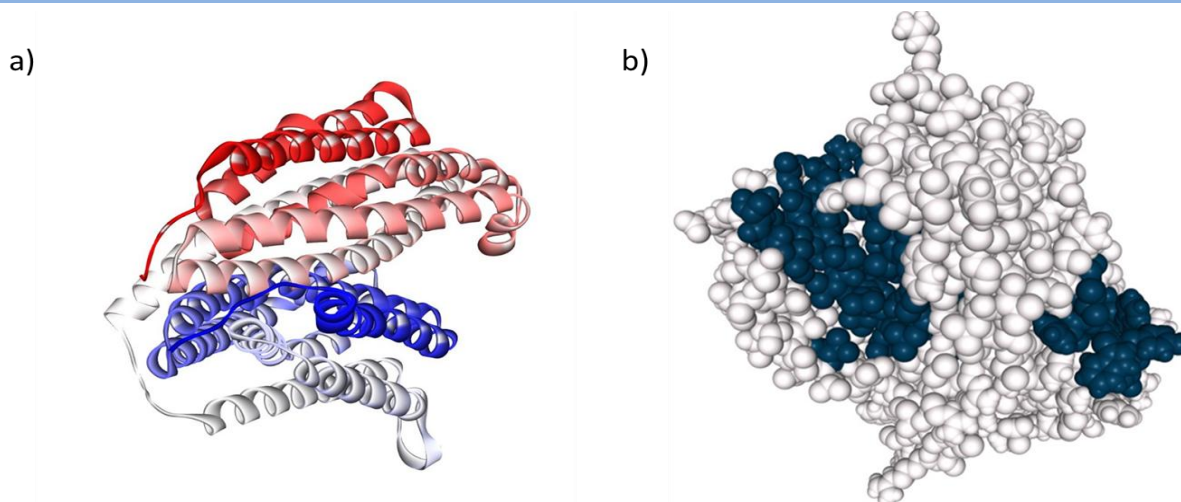


Figure 3 a) probability of residue forming binding site in modelled protein b) Residue depth of modelled protein c) predicted pKa of amino acid residues of modelled protein d) Ramachandran Plot Analysis of Protein Structure Model (MATE transporter protein)

between the template and the target protein, Rv2836c, and identified conserved regions that strongly support using 6FV6 as a template for homology modeling. The conservation of these sequences suggests that the resulting model will enhance our understanding of the structural features of the mycobacterial MATE transporter. This alignment is a foundation for further computational analyses and structural predictions, potentially leading to significant advancements in our understanding of MATE transporter function and developing novel antimicrobial strategies targeting this Protein in mycobacterial species. We prepared the proteins using homology modeling, taking 6FV6 as the template. The three-dimensional structure of the resulting receptor is shown in Figure 2, which displays the MODELLER-modeled MATE transporter protein and an image of the modeled Protein from the DEPTH server.

The protein structure was validated using a Ramachandran plot. According to the plot statistics, 95.4% of the residues are located in favored regions, indicating that the model is of good quality and has accurate protein geometry and conformation, as shown in Figure 3. The presence of only a few outliers in disallowed regions suggests that the overall structural quality is satisfactory. Additionally, the protein structure underwent minimization using SPDBV software to

eliminate clashes. The minimized Protein was then aligned with the original structure to check for significant distortions. Table 1 lists the ligands selected for the study and their corresponding PubChem IDs. These ligands were converted into PDB and PDBQT formats using Open Babel and a Raccoon Python script. This conversion was necessary to prepare the ligands for successful docking experiments.

3.2 Molecular Docking and Screening

The grid was generated using ADT software based on the residues provided by the DEPTH server. The modeled Protein was then docked against known inhibitors of a similar class of proteins, with the exhaustiveness parameter set to 9. Table 1 lists compounds that have demonstrated proven activity against related receptors. In total, 33 compounds were docked, and 28 showed binding affinity toward the transporter protein. Some compounds exhibited structural distortion during docking; however, these results were not considered for further analysis.

Our analysis of the docked compounds identified five potential leads: Hoechst (-11.1 kcal/mol), Zosuquidar (-10.4 kcal/mol), 5'-Methoxyhydnocarbin (5'MHC) (-9.6 kcal/mol), Amitriptylinoxide (-8.7 kcal/mol), and Ethidium Bromide (-8.4 kcal/mol).

Table 1 Activity and Binding Affinity of Docked Compounds

S. N.	Compound name	Activity	Binding affinity (kcal/mol)
1	Zosuquidar (LY335979)	3 rd generation modulators of P-gp inhibit ATP hydrolysis activity	-10.4
2	Hoechst [CID-1464]	Indicate the efflux pump activity in bacteria	-11.1
3	5'-Methoxyhydnocarbin (5'MHC) [CID-5281879]	Inhibits the NorA in <i>S. aureus</i>	-9.6
4	Amitriptylinoxide [CID-20313]	Antibacterial activity	-8.7
5	Amitriptyline [CID-2160]	Inhibit AcrB-mediated efflux by interfering with substrate binding	-7.2
6	Verapamil [CID-2520]	EPI, inhibits <i>M.tuberculosis</i> rifampicin efflux	-5.9
7	Carbonyl Cyanide m-Chlorophenylhydrazone [CID-2603]	Disrupts ATP Synthesis, Interfering with the proton gradient	-7.5
8	Ciprofloxacin [CID-2764]	NorA inhibitor	-6.2
9	4',6-Diamidino-2-phenylindole [CID-2954]	Binds to adenine-thymine-rich regions in DNA	-7.2
10	Ethidium bromide [CID-3624]	Substrate for efflux pumps	-8.4
11	Paroxetine [CID-43815]	inhibits both NorA and MepA	-6.2
12	Reserpine [CID-5770]	Inhibitor of both mammalian and gram-positive bacterial efflux, Inhibit Bmr efflux pump in <i>Bacillus subtilis</i> , NorA pump in <i>S. aureus</i>	-6.7
13	Sertraline [CID-68617]	Inhibit general bacterial efflux pumps	-8.2
14	Citalopram	Potentiate the activity of fluoroquinolones	-7.3
15	Venlafaxine [CID-5656]	Potential efflux pump inhibitor in bacteria	-5.6
16	Escitalopram [CID-146570]	Intrinsic antimicrobial activity against Gram-positive bacteria	-7.5

S. N.	Compound name	Activity	Binding affinity (kcal/mol)
17	Nortriptyline [CID-4543]	Potential efflux pump inhibition	-8.3
18	Trimipramine	Inhibition potencies	-6.3
19	Norfloxacin [CID-4539]	Antimicrobial activity	-7.1
20	Kanamycin [CID-6032]	Inhibiting protein synthesis in bacteria	-7.1
21	Ampicillin [CID-6249]	Beta-lactam antibiotic that inhibits cell wall synthesis	-7.8
22	Acriflavine	Multidrug pump inhibitor	-1.2
23	Rhodamine 6G [CID13807]	Potential efflux pump inhibitor	-6
24	Pyrone Y [CID-7068]	Target cell structures like RNA, DNA, and organelles	-7.8
25	Benzalkonium chloride [CID-8754]	Antibacterial activity	-4.9
26	Triton X-100 [CID-5590]	Inhibits the AcrB transporter	-5.7
27	Crystal violet [CID-3468]	Potential biofilm inhibition	-7.1
28	Berberine [CID-2353]	Inhibits MdfA	-6.2

Figure 4 shows the 3D docking poses of the lead compounds. Among these options, Hoechst, a blue fluorescent dye commonly used for DNA staining, was not selected for further study. Instead, we have chosen Zosuquidar as a candidate due to its significant binding affinity of -10.4 kcal/mol to our modeled protein structure. The docking pose is illustrated in Figure 5. The arrangement of amino acid residues surrounding the ligand indicates a favorable binding pocket or cavity. Key residues such as ILE A.204, GLN A.207, and HIS A.177 likely participate in potential hydrogen bonding interactions, which can enhance the binding affinity and

specificity. Additionally, residues like LEU A.49, MET A.173, and TRP A.63 may play a role in hydrophobic interactions with the non-polar regions of the ligand, further stabilizing the binding complex. Overall, the docking results suggest that the ligand can effectively bind to the Protein's binding pocket, forming specific interactions with critical amino acid residues through both hydrogen bonding and hydrophobic interactions. Based on the docking score of Zosuquidar, the protein-ligand complex was subjected to a 100 ns molecular dynamics simulation to evaluate the ligand's stability within the receptor cavity.

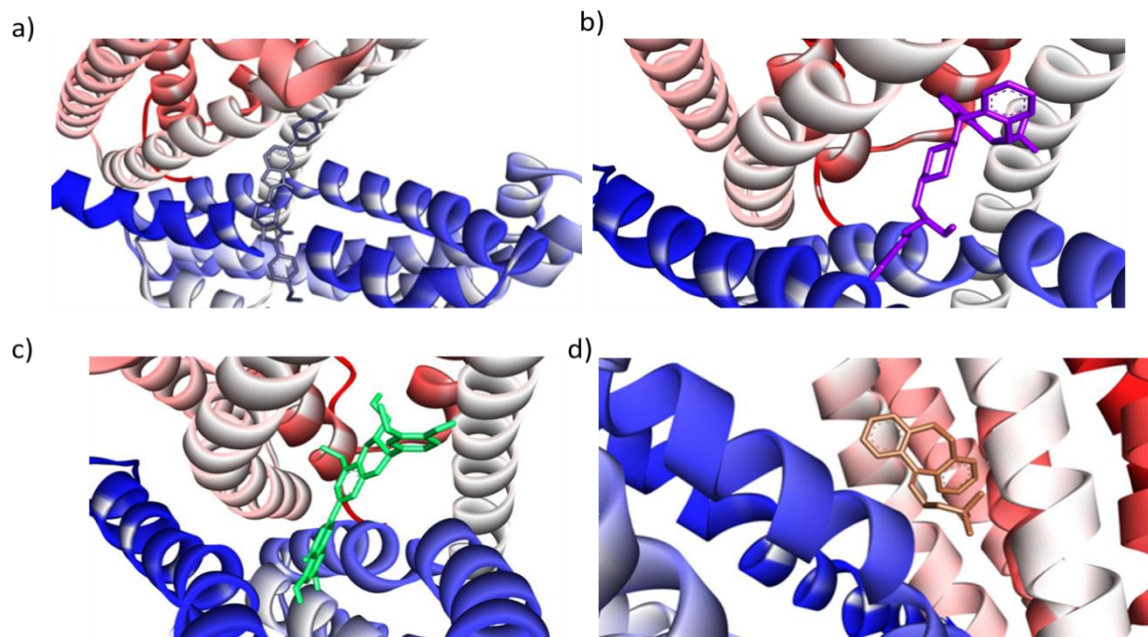


Figure 4 3D docking poses of lead compounds with modelled mycobacterial MATE transporter protein a) Hoechst (-11.1) b) Zosuquidar (-10.4) c) 5' Methoxyhydnoicarpin (-9.6) d) Amitriptylinoxide (-8.7)

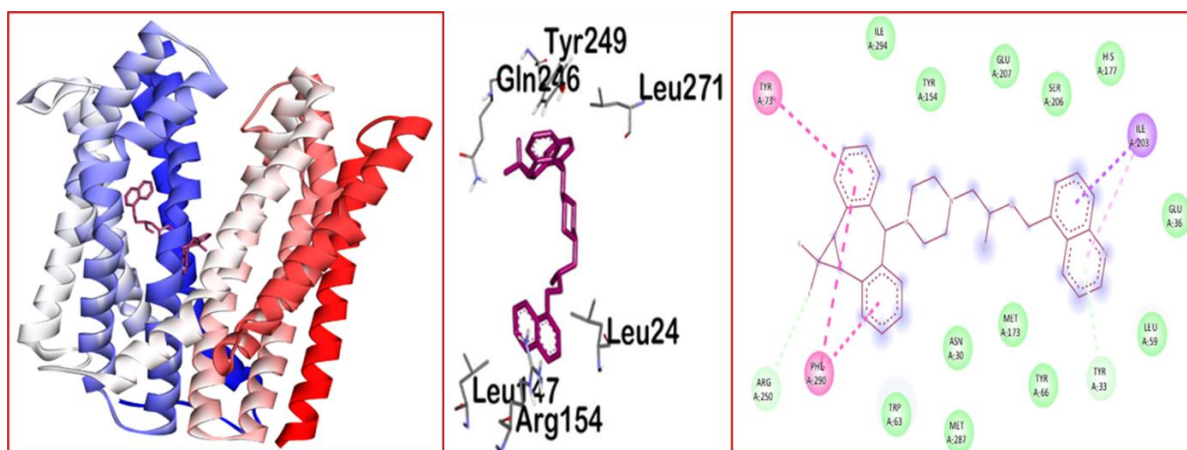


Figure 5 Representation of 3D and 2D binding pose of Zosuquidar bound to modelled MATE transporter protein indicating key binding interactions

3.3 ADMET Analysis of Zosuquidar

The top-ranking compound, Zosuquidar, was evaluated for its ADMET (Absorption, Distribution, Metabolism, Excretion, and Toxicity) properties using the pKCSM server. The predicted ADMET parameters for Zosuquidar show favorable profiles. Its molecular weight is 636.998 g/mol, which is desirable for drug-like compounds, suggesting good membrane permeability and bioavailability potential. The calculated LogP value of 6.5721 indicates relatively high lipophilicity, a factor that can enhance membrane permeability and absorption. Zosuquidar contains six rotatable bonds, contributing to its conformational flexibility and may affect its interactions with the target protein. The compound has five hydrogen bond acceptors and one hydrogen bond donor, indicating the potential for forming favorable interactions within the binding site. The topological polar surface area (TPSA) of 262.662 Å² is relatively high, suggesting greater polarity than typical drug-like compounds. This property can influence solubility, membrane permeability, and the ability to cross the blood-brain barrier. These molecular characteristics provide valuable insights into the compound's drug-like nature and potential pharmacokinetic behavior, aiding in evaluating and optimizing lead candidates in our drug discovery process. Furthermore, the BOILED-Egg model assessed compounds' drug-likeness and gastrointestinal absorption based on their lipophilicity. The LogP values suggest that Zosuquidar has moderate to high lipophilicity, favorable for permeability across biological membranes and potential oral absorption.

3.4 Molecular Dynamics

The protein-drug binding profile of *M. tuberculosis* (Mtb) was obtained through simulations of the drug-receptor complex. Unraveling the dynamic intricacies of these stable interactions sheds light on the nuances of the binding process, contributing to a deeper understanding of the molecular mechanisms that underlie

the drug's efficacy. This comprehensive insight into the dynamic interplay between proteins and drugs could potentially inform targeted drug design strategies for more effective therapeutics.

3.5 Unravelling Complex Formation: Insights into Binding Dynamics and Stability

The trajectory of the protein-drug complex was systematically analyzed to evaluate the stability of these complexes within a solvent-rich dynamic environment, using Root Mean Square Deviation (RMSD) as a measure. We conducted a comparative assessment of the RMSD values for the complex and the Protein in the absence of the drug to estimate the effectiveness of complex formation and its ability to maintain stability throughout the 100 ns simulations. Figure 6a shows that the drug remained in the binding site and maintained complex stability over the 100 ns simulations, with an average RMSD of 0.3016 nm. A slight decrease in fluctuations was noted between 49 and 58 ns. Further examination of the trajectory revealed that this minor drop in fluctuations could be attributed to a slight change in the conformation of the drug within the binding site.

The Radius of Gyration (Rg) was calculated to evaluate the effect of drug binding on the structural compactness of the mycobacterial MATE transporter. The results showed minor differences in Rg values for tRNA, both with and without the drug, ranging from 0.3 to 0.5 nm (Figure 6b). These findings indicate that drug binding caused slight structural changes, which affected the overall shape and increased the structural compactness of the receptor, ultimately contributing to its stability.

3.6 Root Mean Square Fluctuations

The root mean square fluctuations (RMSF) of the base pairs in the mycobacterial MATE transporter were systematically evaluated to understand the drug's impact on their flexibility and stability. The

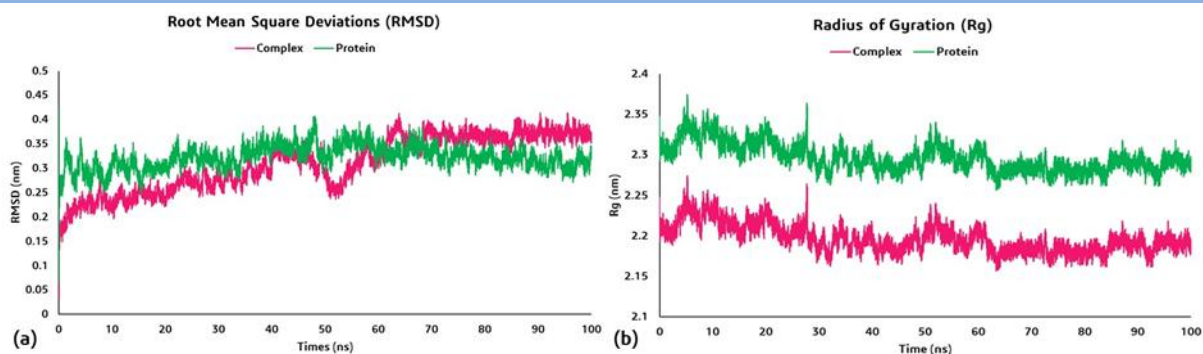


Figure 6a) Root Mean Square Deviations (RMSD), b) Radius of Gyration (Rg)

Root Mean Square Fluctuations

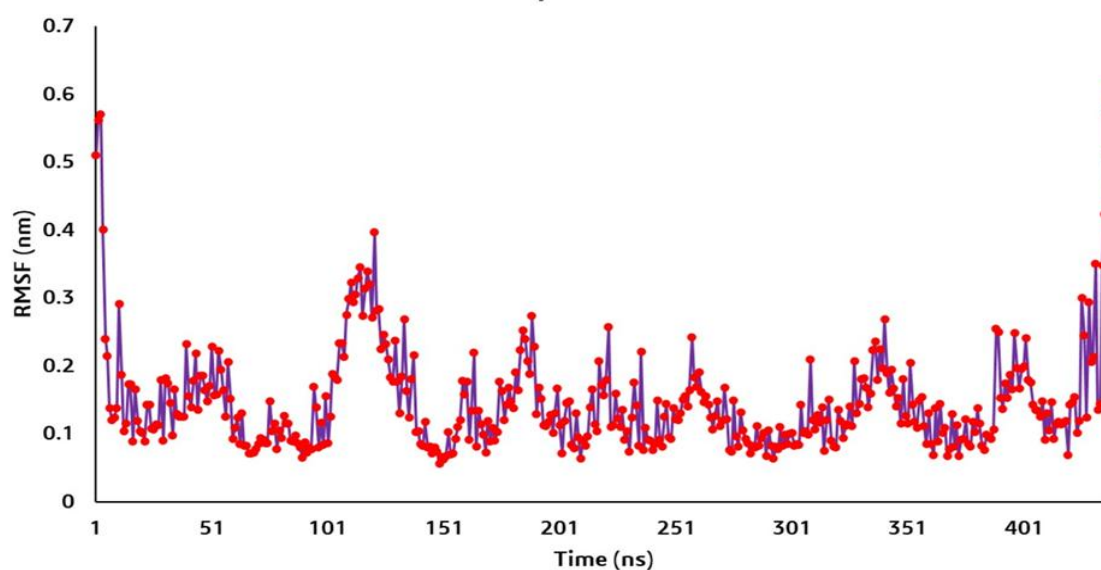


Figure 7 This graph represents the structural flexibility of MATE transporter protein during the simulation, Root Mean Square Fluctuations (RMSF). Higher RMSF values indicate greater flexibility or movement in specific regions or time points.

results indicated that upon binding to the receptor, the drug significantly decreased the flexibility of the base pairs, leading to increased interactions and promoting the formation of a stable complex (Figure 7). Notably, minor fluctuations were observed in some areas of *M. tuberculosis* (Mtb), particularly in the loops and random coils of the secondary structure. However, these fluctuations were likely due to the dynamic nature of the environment rather than direct interactions with the drug. In contrast, amino acid residues within the binding domain showed reduced fluctuations, indicating their active role in forming stable interactions with the drug. This finding suggests that these residues are crucial in decreasing flexibility, thus enhancing the stability of the protein-drug complex.

3.7 Investigation of Key Binding Interactions

The trajectories were further analyzed to evaluate the drug's binding mode and interactions with the mycobacterial MATE

transporter protein. A visual inspection of the protein-drug complex trajectory revealed that the initial binding site was consistently maintained throughout the trajectory, with only minor changes in the drug's conformation within the binding site (Figure 8). Stable hydrophobic interactions were observed in the complex. The higher hydrophobicity of drugs with multiple aromatic rings may contribute to these hydrophobic interactions.

3.8 Energy Evaluation of the Complexation

The trajectories of the MATE protein-drug complex were systematically analyzed to determine the binding free energy of the complex. Notably, the primary contributors to the binding free energies were van der Waals interactions, solvent effects, Poisson-Boltzmann (PB) energies, and non-polar energies (Table 2). The total binding free energy for the protein-ligand complex was -8.54 kcal/mol, indicating a favorable and strong drug-binding interaction with the multidrug transporter. The van der Waals interactions were

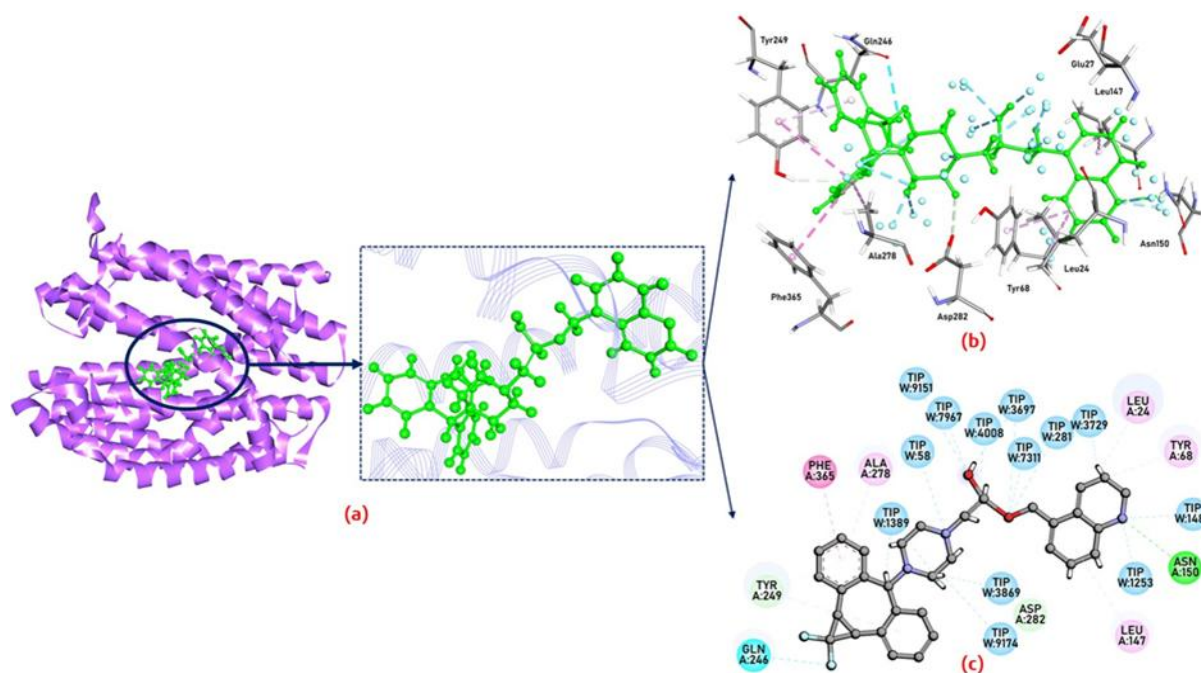


Figure 8 illustrates the binding interaction between a MATE transporter protein and the drug zosuquidar. It comprises three interconnected panels: (a) A broad view of the protein-drug complex. The transporter protein is depicted in purple using a ribbon representation, showing its overall secondary structure. The bound zosuquidar molecule is highlighted in green within a dark circular outline, nestled in a binding pocket of the Protein, (b) An enlarged view of the binding site, detailing the molecular interactions between Zosuquidar (green) and the surrounding amino acid residues of the Protein (gray). Dotted lines indicate potential hydrogen bonds or other non-covalent interactions. Key amino acid residues are labelled, (c) A 2D schematic representation of the binding site. It shows the chemical structure of Zosuquidar (in black) surrounded by interacting amino acid residues. These residues are depicted as coloured circles with their three-letter codes and position numbers. The colour coding represents different types of amino acids or their roles in the interaction.

Table 2 Binding free energy components for the protein-ligand complex calculated using MM/PBSA

Binding Free Energy	Complex (kcal/mol)
Electrostatic (Elec)	8.2202
Van der Waals (Vdw)	-41.6351
Polar Solvation (PB)	28.9779
Non-polar Solvation (SA)	-4.103
Gas Phase Energy (Gas)	-33.4149
Solvation Free Energy (Sol)	24.8749
Polar Contribution (Pol)	37.198
Non-polar Contribution (Npol)	-45.738
Total Binding Free Energy	-8.54

major contributors to this binding affinity, which accounted for -41.64 kcal/mol. This suggests that hydrophobic interactions play a critical role in stabilizing the complex. Breaking down the components of the binding free energy provides valuable insights into the forces governing the protein-ligand interactions. The significant contribution from van der Waals interactions and a favorable non-polar solvation term indicate that hydrophobic

effects and structural complementarity primarily drive the binding. These binding free energy calculations, combined with molecular docking and dynamics simulations, offer a comprehensive understanding of the binding mechanisms and assist in optimizing Zosuquidar as a potent inhibitor targeting the mycobacterial MATE transporter protein. The sequence of the multidrug transporter was threaded to known structural templates using

MODBASE, which generated comparative models. The highest-scoring model was refined through energy minimization in SPDBV. Cavity detection, performed using the DEPTH server, identified potential drug-binding regions. A focused library of twenty-eight reported efflux pump inhibitors, including Zosuquidar, was docked against the MATE transporter model using AutoDock Tools. Ligands were prepared in BIOVIA Discovery Studio by generating isomers and ionization variants at a pH of 7.0 ± 2.0 . Polar hydrogens were added to the prepared multidrug transporter structure, and partial charges were assigned using the Gasteiger method before generating the docking grid focused on the detected cavity. Autodock Vina executed rigid dockings with an exhaustiveness level of 9, providing predicted free energies and binding poses. The top-scoring compound, Zosuquidar, exhibited a favorable predicted affinity of -10.4 kcal/mol. This complex subsequently underwent explicit-solvent molecular dynamics simulations using Amberleap with the ff14SB force field, neutralized with NaCl ions. After minimization and equilibration, a 100 ns production simulation was conducted with NAMD 2.14 under constant 310 K temperature and 1 bar pressure. An ensemble of 2500 trajectory snapshots was generated for analysis using cpptraj. Key metrics, including root mean square deviation (RMSD), hydrogen bonds, and solvent accessibility, were assessed to evaluate binding stability and identify interacting residues.

Zosuquidar is an efflux pump inhibitor that targets P-glycoprotein and ABC transporters, which play a crucial role in multidrug resistance in cancer. Sandler et al. (2004) studied the safety and tolerability of combining Zosuquidar with doxorubicin in patients with advanced malignancies. Another study by Morrish et al. (2020) showed that Zosuquidar inhibits Hepatitis B Virus (HBV) replication in liver cells when combined with birinapant. As an ABC efflux pump inhibitor, Zosuquidar shows promise in reversing transporter-mediated chemoresistance, as highlighted by Robey et al. (2018). This compound increases drug accumulation in tumors expressing P-glycoproteins, improving etoposide absorption, especially when paired with non-ionic surfactants (Nielsen et al. 2023). Additionally, Zosuquidar has been observed to inhibit multidrug-resistant bacterial strains, including *Acinetobacter baumannii* and *E. coli* (Cripe et al. 2010; Alenazy 2022; Pelegrinova et al. 2024). It also increases the efficacy of polymyxins by enhancing bacterial susceptibility, which underscores its potential as an antibiotic adjuvant (Turner et al. 2020). Our findings suggest that Zosuquidar could be repurposed as an efflux pump inhibitor targeting Rv2836c. This is supported by a previous study indicating that sertraline can inhibit mycobacterial efflux activity, significantly enhancing the potency of bedaquiline (Shankaran et al. 2023). Multidrug transporters in mycobacteria are believed to significantly contribute to antimicrobial resistance (Srivastav et al. 2019; Datta et al. 2024).

Transporters like Rv2836c in *M. tuberculosis* (Mtb) are known to extrude various drugs and antimicrobials (Mishra and Daniels 2013; Long et al. 2024). The overexpression of these genes has been demonstrated to promote fluoroquinolone efflux, thereby reducing drug efficacy in multidrug-resistant tuberculosis (Kim et al. 2021). Environmental factors and exposure to sublethal antibiotic doses can upregulate these multidrug transporters, enhancing bacterial resistance (Spengler et al. 2017; Machado et al. 2017; Miotto et al. 2022).

Despite existing research, the potential of Zosuquidar as an efflux pump inhibitor in bacteria has not been fully explored. This study evaluated its activity as a potential inhibitor targeting the mycobacterial multidrug transporter. We investigated its binding affinity and inhibitory potential against the mycobacterial efflux transporter using molecular docking and molecular dynamics. The protein structure was modeled using homology and docked with Zosuquidar, predicting a strong binding affinity at the drug-binding pocket, where we identified significant interactions responsible for the stability of the complex. The simulation indicates that Zosuquidar maintains stable binding while reducing transporter flexibility, suggesting potential allosteric inhibition.

Conclusions

Our analysis identifies various binding modes and key sites on the MATE transporter, enhancing our understanding of the mechanisms behind efflux pump inhibition. We characterized the molecular interactions that could impact the efficacy of the inhibitors. This study offers new insights into inhibiting the mycobacterial MATE efflux transporter. Further research is necessary to assess the effectiveness of these inhibitors against mycobacterial efflux pumps to tackle multidrug and antimicrobial resistance.

Acknowledgments

The authors thank Amity University for providing all facilities and infrastructural support. AR and RS acknowledge the DST INSPIRE Faculty Fellowship.

Data Availability Statement

All the data generated during the work has been provided in the manuscript.

Funding Declaration

No funding received.

Clinical Trial number

Not Applicable

Conflicts of Interest

No conflicts

Ethical Clearance

Not Applicable

References

Alenazy R. (2022). Drug Efflux Pump Inhibitors: A Promising Approach to Counter Multidrug Resistance in Gram-Negative Pathogens by Targeting AcrB Protein from AcrAB-TolC Multidrug Efflux Pump from *Escherichia coli*. *Biology*, *11*(9), 1328. <https://doi.org/10.3390/biology11091328>.

Andre, E., Goeminne, L., Cabibbe, A., Beckert, P., Kabamba Mukadi, B., et al. (2017). Consensus numbering system for the rifampicin resistance-associated rpoB gene mutations in pathogenic mycobacteria. *Clinical microbiology and infection: the official publication of the European Society of Clinical Microbiology and Infectious Diseases*, *23*(3), 167–172. <https://doi.org/10.1016/j.cmi.2016.09.006>.

Athar, M., Gervasoni, S., Catte, A., Basciu, A., Mallocci, G., Ruggerone, P., & Vargiu, A. V. (2023). Tripartite efflux pumps of the RND superfamily: what did we learn from computational studies?. *Microbiology (Reading, England)*, *169*(3), 001307. <https://doi.org/10.1099/mic.0.001307>.

Black, P. A., Warren, R. M., Louw, G. E., van Helden, P. D., Victor, T. C., & Kana, B. D. (2014). Energy metabolism and drug efflux in *Mycobacterium tuberculosis*. *Antimicrobial agents and chemotherapy*, *58*(5), 2491–2503. <https://doi.org/10.1128/AAC.02293-13>.

Campolattano, N., D'Abrosca, G., Russo, L., De Siena, B., Della Gala, M., et al. (2023). Insight into the on/off switch that regulates expression of the MSMEG-3762/63 efflux pump in *Mycobacterium smegmatis*. *Scientific reports*, *13*(1), 20332. <https://doi.org/10.1038/s41598-023-47695-4>.

Cripe, L. D., Uno, H., Paietta, E. M., Litzow, M. R., Ketterling, R. P., et al. (2010). Zosuquidar, a novel modulator of P-glycoprotein, does not improve the outcome of older patients with newly diagnosed acute myeloid leukemia: a randomized, placebo-controlled trial of the Eastern Cooperative Oncology Group 3999. *Blood*, *116*(20), 4077–4085. doi:10.1182/blood-2010-04-277269

Datta, D., Jamwal, S., Jyoti, N., Patnaik, S., & Kumar, D. (2024). Actionable mechanisms of drug tolerance and resistance in *Mycobacterium tuberculosis*. *The FEBS journal*, *291*(20), 4433–4452. <https://doi.org/10.1111/febs.17142>.

Day, N. J., Santucci, P., & Gutierrez, M. G. (2024). Host cell environments and antibiotic efficacy in tuberculosis. *Trends in microbiology*, *32*(3), 270–279. <https://doi.org/10.1016/j.tim.2023.08.009>.

Forli, S., Huey, R., Pique, M. E., Sanner, M. F., Goodsell, D. S., & Olson, A. J. (2016). Computational protein-ligand docking and virtual drug screening with the AutoDock suite. *Nature protocols*, *11*(5), 905–919. <https://doi.org/10.1038/nprot.2016.051>.

Ghajavand, H., Kargarpour Kamakoli, M., Khanipour, S., Pourazar Dizaji, S., Masoumi, M., et al. (2019). Scrutinizing the drug resistance mechanism of multi- and extensively-drug resistant *Mycobacterium tuberculosis*: mutations versus efflux pumps. *Antimicrobial resistance and infection control*, *8*, 70. <https://doi.org/10.1186/s13756-019-0516-4>.

Goletti, D., Meintjes, G., Andrade, B. B., Zumla, A., & Shan Lee, S. (2025). Insights from the 2024 WHO Global Tuberculosis Report - More Comprehensive Action, Innovation, and Investments required for achieving WHO End TB goals. *International journal of infectious diseases : IJID : official publication of the International Society for Infectious Diseases*, *150*, 107325. <https://doi.org/10.1016/j.ijid.2024.107325>.

Gopi, P., Gurnani, M., Singh, S., Sharma, P., & Pandya, P. (2023). Structural aspects of SARS-CoV-2 mutations: Implications to plausible infectivity with ACE-2 using computational modeling approach. *Journal of biomolecular structure & dynamics*, *41*(14), 6518–6533. <https://doi.org/10.1080/07391102.2022.2108901>.

Hassan, K. A., Liu, Q., Elbourne, L. D. H., Ahmad, I., Sharples, D., et al. (2018). Pacing across the membrane: the novel PACE family of efflux pumps is widespread in Gram-negative pathogens. *Research in microbiology*, *169*(7-8), 450–454. <https://doi.org/10.1016/j.resmic.2018.01.001>.

Henderson, P. J. F., Maher, C., Elbourne, L. D. H., Eijkelkamp, B. A., Paulsen, I. T., & Hassan, K. A. (2021). Physiological Functions of Bacterial "Multidrug" Efflux Pumps. *Chemical reviews*, *121*(9), 5417–5478. <https://doi.org/10.1021/acs.chemrev.0c01226>.

Huang, L., Wu, C., Gao, H., Xu, C., Dai, M., Huang, L., Hao, H., Wang, X., & Cheng, G. (2022). Bacterial Multidrug Efflux Pumps at the Frontline of Antimicrobial Resistance: An Overview. *Antibiotics (Basel, Switzerland)*, *11*(4), 520. <https://doi.org/10.3390/antibiotics11040520>.

Humphrey, W., Dalke, A., & Schulten, K. (1996). VMD: visual molecular dynamics. *Journal of molecular graphics*, *14*(1), 33–28. [https://doi.org/10.1016/0263-7855\(96\)00018-5](https://doi.org/10.1016/0263-7855(96)00018-5).

- Kim, J., Cater, R. J., Choy, B. C., & Mancina, F. (2021). Structural Insights into Transporter-Mediated Drug Resistance in Infectious Diseases. *Journal of molecular biology*, 433(16), 167005. <https://doi.org/10.1016/j.jmb.2021.167005>.
- Klukovits, A., & Krajcsi, P. (2015). Mechanisms and therapeutic potential of inhibiting drug efflux transporters. *Expert opinion on drug metabolism & toxicology*, 11(6), 907–920. <https://doi.org/10.1517/17425255.2015.1028917>.
- Lee, J., Cheng, X., Swails, J. M., Yeom, M. S., Eastman, P. K., et al. (2016). CHARMM-GUI Input Generator for NAMD, GROMACS, AMBER, OpenMM, and CHARMM/OpenMM Simulations Using the CHARMM36 Additive Force Field. *Journal of chemical theory and computation*, 12(1), 405–413. <https://doi.org/10.1021/acs.jctc.5b00935>.
- Long, Y., Wang, B., Xie, T., Luo, R., Tang, J., Deng, J., & Wang, C. (2024). Overexpression of efflux pump genes is one of the mechanisms causing drug resistance in *Mycobacterium tuberculosis*. *Microbiology spectrum*, 12(1), e0251023. <https://doi.org/10.1128/spectrum.02510-23>.
- Machado, D., Coelho, T. S., Perdigão, J., Pereira, C., Couto, I., Portugal, I., Maschmann, R. A., Ramos, D. F., von Groll, A., Rossetti, M. L. R., Silva, P. A., & Viveiros, M. (2017). Interplay between Mutations and Efflux in Drug Resistant Clinical Isolates of *Mycobacterium tuberculosis*. *Frontiers in microbiology*, 8, 711. <https://doi.org/10.3389/fmicb.2017.00711>.
- Maphasa, R. E., Meyer, M., & Dube, A. (2021). The Macrophage Response to *Mycobacterium tuberculosis* and Opportunities for Autophagy Inducing Nanomedicines for Tuberculosis Therapy. *Frontiers in cellular and infection microbiology*, 10, 618414. <https://doi.org/10.3389/fcimb.2020.618414>.
- Miotto, P., Sorrentino, R., De Giorgi, S., Provvedi, R., Cirillo, D. M., & Manganelli, R. (2022). Transcriptional regulation and drug resistance in *Mycobacterium tuberculosis*. *Frontiers in cellular and infection microbiology*, 12, 990312. <https://doi.org/10.3389/fcimb.2022.990312>.
- Mishra, M. N., & Daniels, L. (2013). Characterization of the MSMEG_2631 gene (mmp) encoding a multidrug and toxic compound extrusion (MATE) family protein in *Mycobacterium smegmatis* and exploration of its polyspecific nature using biologic phenotype microarray. *Journal of bacteriology*, 195(7), 1610–1621. <https://doi.org/10.1128/JB.01724-12>.
- Monedero-Recuero, I., Gegia, M., Wares, D. F., Chadha, S. S., & Mirzayev, F. (2021). Situational analysis of 10 countries with a high burden of drug-resistant tuberculosis 2 years post-UNHLM declaration: progress and setbacks in a changing landscape. *International journal of infectious diseases : IJID : official publication of the International Society for Infectious Diseases*, 108, 557–567. <https://doi.org/10.1016/j.ijid.2021.06.022>.
- Morrish, E., Mackiewicz, L., Silke, N., Pellegrini, M., Silke, J., Brumatti, G., & Ebert, G. (2020). Combinatorial Treatment of Birinapant and Zosuquidar Enhances Effective Control of HBV Replication In Vivo. *Viruses*, 12(8), 901. <https://doi.org/10.3390/v12080901>.
- Nielsen, R. B., Holm, R., Pijpers, I., Snoeys, J., Nielsen, U. G., & Nielsen, C. U. (2023). Combinational Inhibition of P-Glycoprotein-Mediated Etoposide Transport by Zosuquidar and Polysorbate 20. *Pharmaceutics*, 15(1), 283. <https://doi.org/10.3390/pharmaceutics15010283>.
- O'Boyle, N. M., Banck, M., James, C. A., Morley, C., Vandermeersch, T., & Hutchison, G. R. (2011). Open Babel: An open chemical toolbox. *Journal of cheminformatics*, 3, 33. <https://doi.org/10.1186/1758-2946-3-33>.
- Peddireddy, V., Doddam, S. N., & Ahmed, N. (2017). Mycobacterial Dormancy Systems and Host Responses in Tuberculosis. *Frontiers in immunology*, 8, 84. <https://doi.org/10.3389/fimmu.2017.00084>.
- Pelegriņova, L., Sofrankova, L., Spaldova, J., Stefik, P., Sulova, Z., Breier, A., & Elefantova, K. (2024). Zosuquidar: An Effective Molecule for Intracellular Ca²⁺ Measurement in P-gp Positive Cells. *International journal of molecular sciences*, 25(6), 3107. <https://doi.org/10.3390/ijms25063107>.
- Phillips, J. C., Hardy, D. J., Maia, J. D. C., Stone, J. E., Ribeiro, J. V., et al. (2020). Scalable molecular dynamics on CPU and GPU architectures with NAMD. *The Journal of chemical physics*, 153(4), 044130. <https://doi.org/10.1063/5.0014475>.
- Poulton, N. C., & Rock, J. M. (2022). Unraveling the mechanisms of intrinsic drug resistance in *Mycobacterium tuberculosis*. *Frontiers in cellular and infection microbiology*, 12, 997283. <https://doi.org/10.3389/fcimb.2022.997283>.
- Roberts A. G. (2021). The Structure and Mechanism of Drug Transporters. *Methods in molecular biology (Clifton, N.J.)*, 2342, 193–234. https://doi.org/10.1007/978-1-0716-1554-6_8.
- Robey, R. W., Pluchino, K. M., Hall, M. D., Fojo, A. T., Bates, S. E., & Gottesman, M. M. (2018). Revisiting the role of ABC transporters in multidrug-resistant cancer. *Nature reviews. Cancer*, 18(7), 452–464. <https://doi.org/10.1038/s41568-018-0005-8>.
- Rodrigues, L., Cravo, P., & Viveiros, M. (2020). Efflux pump inhibitors as a promising adjunct therapy against drug resistant

- tuberculosis: a new strategy to revisit mycobacterial targets and repurpose old drugs. *Expert review of anti-infective therapy*, 18(8), 741–757. <https://doi.org/10.1080/14787210.2020.1760845>.
- Rodrigues, L., Cravo, P., & Viveiros, M. (2020). Efflux pump inhibitors as a promising adjunct therapy against drug resistant tuberculosis: a new strategy to revisit mycobacterial targets and repurpose old drugs. *Expert review of anti-infective therapy*, 18(8), 741–757. <https://doi.org/10.1080/14787210.2020.1760845>.
- Seung, K. J., Keshavjee, S., & Rich, M. L. (2015). Multidrug-Resistant Tuberculosis and Extensively Drug-Resistant Tuberculosis. *Cold Spring Harbor perspectives in medicine*, 5(9), a017863. <https://doi.org/10.1101/cshperspect.a017863>.
- Chang, D. P. S., & Guan, X. L. (2021). Metabolic Versatility of *Mycobacterium tuberculosis* during Infection and Dormancy. *Metabolites*, 11(2), 88. <https://doi.org/10.3390/metabo11020088>.
- Shankaran, D., Singh, A., Dawa, S., Arumugam, P., Gandotra, S., & Rao, V. (2023). The antidepressant sertraline provides a novel host directed therapy module for augmenting TB therapy. *eLife*, 12, e64834. <https://doi.org/10.7554/eLife.64834>.
- Sharma, K., Ahmed, F., Sharma, T., Grover, A., Agarwal, M., & Grover, S. (2023). Potential Repurposed Drug Candidates for Tuberculosis Treatment: Progress and Update of Drugs Identified in Over a Decade. *ACS omega*, 8(20), 17362–17380. <https://doi.org/10.1021/acsomega.2c05511>.
- Spengler, G., Kincses, A., Gajdács, M., & Amaral, L. (2017). New Roads Leading to Old Destinations: Efflux Pumps as Targets to Reverse Multidrug Resistance in Bacteria. *Molecules*, 22 (3), 468. <https://doi.org/10.3390/molecules22030468>.
- Srivastav, R., Kumar, D., Grover, A., Singh, A., Manjasetty, B. A., Sharma, R., & Taneja, B. (2014). Unique subunit packing in mycobacterial nanoRNase leads to alternate substrate recognitions in DHH phosphodiesterases. *Nucleic acids research*, 42(12), 7894–7910. <https://doi.org/10.1093/nar/gku425>.
- Srivastav, R., Sharma, R., Tandon, S., & Tandon, C. (2019). Role of DHH superfamily proteins in nucleic acids metabolism and stress tolerance in prokaryotes and eukaryotes. *International journal of biological macromolecules*, 127, 66–75. <https://doi.org/10.1016/j.ijbiomac.2018.12.123>.
- Traoré, A. N., Rikhotso, M. C., Mphaphuli, M. A., Patel, S. M., Mahamud, H. A., Kachienga, L. O., Kabue, J. P., & Potgieter, N. (2023). Isoniazid and Rifampicin Resistance-Confering Mutations in *Mycobacterium tuberculosis* Isolates from South Africa. *Pathogens (Basel, Switzerland)*, 12(8), 1015. <https://doi.org/10.3390/pathogens12081015>.
- Turner, A. P., Alam, C., & Bendayan, R. (2020). Efflux Transporters in Cancer Resistance: Molecular and Functional Characterization of P-Glycoprotein. In A. Sosnik, & R. Bendayan (Eds.) *Drug Efflux Pumps in Cancer Resistance Pathways: From Molecular Recognition and Characterization to Possible Inhibition Strategies in Chemotherapy, Cancer Sensitizing Agents for Chemotherapy* vol. 7 (pp. 1–30). Academic Press. <https://doi.org/https://doi.org/10.1016/B978-0-12-816434-1.00001-2>.
- Tyagi, R., Srivastava, M., Jain, P., Pandey, R. P., Asthana, S., Kumar, D., & Raj, V. S. (2022). Development of potential proteasome inhibitors against *Mycobacterium tuberculosis*. *Journal of biomolecular structure & dynamics*, 40(5), 2189–2203. <https://doi.org/10.1080/07391102.2020.1835722>.
- WHO. (2024). *Global Tuberculosis Report 2024*. Retrieved from <https://www.who.int/teams/global-tuberculosis-programme/tb-reports/global-tuberculosis-report-2024>.
- WHO Results Report 2020-2021. n.d. Retrieved from <https://www.who.int/about/accountability/results/who-results-report-2020-2021>. Accessed February 19, 2024.
- Wilczek, N. A., Brzyska, A., Bogucka, J., Sielwanowska, W. E., Żybowska, M., Pieciewicz-Szczęśna, H., & Smoleń, A. (2023). The Impact of the War in Ukraine on the Epidemiological Situation of Tuberculosis in Europe. *Journal of clinical medicine*, 12(20), 6554. <https://doi.org/10.3390/jcm12206554>.
- Yang, J., Zhang, L., Qiao, W., & Luo, Y. (2023). *Mycobacterium tuberculosis*: Pathogenesis and therapeutic targets. *MedComm*, 4(5), e353. <https://doi.org/10.1002/mco2.353>.
- Zgurskaya H. I. (2021). Introduction: Transporters, Porins, and Efflux Pumps. *Chemical reviews*, 121(9), 5095–5097. <https://doi.org/10.1021/acs.chemrev.1c00010>.
- Zhao, J., Xie, H., Mehdipour, A. R., Safarian, S., Ermler, U., et al. (2021). The structure of the *Aquifex aeolicus* MATE family multidrug resistance transporter and sequence comparisons suggest the existence of a new subfamily. *Proceedings of the National Academy of Sciences of the United States of America*, 118(46), e2107335118. <https://doi.org/10.1073/pnas.2107335118>.